



Pergamon

Available online at www.sciencedirect.com

SCIENCE @ DIRECT®



Acta Materialia 51 (2003) 5063–5071

www.actamat-journals.com

Ferroelasticity in mixed conducting LaCoO_3 based perovskites: a ferroelastic phase transition

Nina Orlovskaya^{a,*}, Nigel Browning^b, Alan Nicholls^c

^a Department of Materials Science and Engineering, Drexel University, 3141 Chestnut Street, Philadelphia, PA 19104, USA

^b University of California Davis, Department of Chemical Engineering and Materials Science, One Shields Ave., Davis, CA 95616, USA

^c University of Illinois at Chicago, Research Resources Center-East (m/c 337), 845 West Taylor Street, Chicago, IL 60607, USA

Received 7 April 2003; received in revised form 18 June 2003; accepted 19 June 2003

Abstract

The defect structure of LaCoO_3 based ferroic perovskites has been studied by TEM. The dynamics of the temperature-induced ferroelastic to paraelastic phase transition was directly monitored by in-situ TEM during thermal cycles from room temperature to 700 °C. Different types of structural features of LaCoO_3 based perovskites have been observed, such as twins, antiphase domains, stacking faults, and dislocations. Domain motion and de-twinning during heating, and the reappearance of twins during cooling have been demonstrated. This is important for the understanding of ferroelastic hysteretic behavior of LaCoO_3 based perovskite ceramics.

© 2003 Acta Materialia Inc. Published by Elsevier Ltd. All rights reserved.

Keywords: Perovskites; Twins; Phase transformation; Ferroelasticity; TEM

1. Introduction

The term “ferroelasticity” was introduced by Aizu [1] for crystals where the stress-strain behavior exhibits a hysteresis that is characterized by spontaneous strain and coercive stress [2,3], while so called “paraelastic” crystals exhibit a linear stress-strain behavior with no hysteresis loop. There are two ingredients that make a crystal ferroelastic:

1. A phase transition between the paraelastic high temperature high symmetry phase and ferroelastic low temperature low symmetry phase. This ferroelastic phase transition creates a lattice distortion.
2. This lattice distortion can be reoriented by an external mechanical stress.

This type of phase transition, which is accompanied by a change of the point-group symmetry, is called a ferroic phase transition [4]. Ferroelectric and ferromagnetic materials are typical examples of ferroics, and ferroelastic materials are simply the mechanical analogues of ferroelectrics and ferromagnetics. In a ferroelastic phase tran-

* Corresponding author. Tel.: +1 215 895 1541; fax: +1 215 895 6760.

E-mail address: orlovsk@drexel.edu (N. Orlovskaya).

sition, the change of point-group symmetry is accompanied by the onset or disappearance of spontaneous strain; a polar, symmetric, second-rank tensor property. Thus, ferroelasticity is associated with the occurrence of spontaneous strain; spontaneous because it has a nonzero magnitude even when no external force is applied to the crystal. The spontaneous strain is measured as the volume average of the structural deformation of the unit cell. It is defined as to be [5]:

- independent of the choice of the coordinate system;
- the same in all the orientation states in the ferroelastic phase;
- zero over the whole temperature range in the prototypic phase.

The spontaneous strain in ferroelastic materials is strongly influenced by the domain structure of the crystal. The domain/twin structure is a consequence of a transformation from the paraelastic phase to the ferroelastic phase and, thus, domains/twins are the dominant microstructure of this low symmetry phase. Domains/twins can coexist in a ferroic crystal because they are energetically equivalent, and because the crystal can minimize its free energy by splitting into an optimum number of domains. In some ferroelastic phases resulting from discontinuous phase transitions, a dense network of domains can provide a stress accommodating mechanism [6]. When stress is applied to a twinned crystal, one direction of the domains/twins remains stable and displays classical elastic behavior, whereas the second direction of the domains/twins is unstable and collapses into the first one when the critical stress is surpassed. If the direction of stress is reversed, the second structural state is stable and the first collapses into the second. This process is called a domain switching/reorientation. The quantity that characterizes the size of the ferroelastic hysteresis is the stress that is necessary to reorient or destroy the domain/twin pattern.

One class of materials where developing a fundamental understanding of ferroelasticity is crucial is in perovskite type ABO_3 (where $A = \text{La, Sr, Ca}$; $B = \text{Co}$) mixed ionic and electronic conducting

(MIEC) ceramics. In particular, lanthanum cobaltite based perovskites are important agile and multifunctional materials, which are very promising for high temperature oxygen separation membranes and cathodes in solid oxide fuel cells (SOFCs) [7,8]. When the B ions can take a mixed valence state, such as in transition metals, the partial substitution of A site cations by other metal cations with lower valences usually causes the formation of oxygen vacancies and a change in the valence state of the B ions in order to maintain the charge neutrality [9]. Substituting ions of similar size but lower valence at the B site can also increase the concentration of oxygen vacancies. The so-called mixed conductors may show both a high oxygen ionic conductivity due to high oxygen vacancy concentration, and a high electronic conductivity due to the mixed-valence state [10].

Despite a number of publications concerning the spin-state [11–13], electrical and magnetic transitions [14–17], and the oxygen permeability of MIEC perovskites [18–20], just a few papers have been published on the ferroelasticity and elastic hysteresis of these materials [21–23]. What is known about these materials is that during fabrication and operation, both the layered SOFC structure and oxygen separation membranes are subject to various thermal cycles, when the large thermal stresses can cause the cracking and failure of the ceramics. The ferroelastic transition was not accounted in the modeling and in the experimental measuring of the residual stresses arising in SOFCs during the fabrication or operation [24]. However, the work on large strain electromechanical actuators with perovskite related structure has shown that the domain switching/phase transition can result in cracking due to the inevitable strain incompatibilities in polycrystalline materials. When LaCoO_3 based ceramics are to be used as solid electrolytes and membranes, cracking of this nature, caused by thermal cycling through the transformation could seriously compromise the membranes.

The application of the physical concepts of ferroelasticity to MIEC perovskites is new and fundamental research on the underlying physical principles, which generate elastic instabilities, is required to understand fully the materials behavior.

A basic understanding of the origin of ferroelastic properties is not currently available for lanthanum cobaltites and other mixed conductors. Here we publish the results of our study of the ferroelasticity in LaCoO_3 based ceramics. In the first part of the publication the TEM study on the paraelastic to ferroelastic phase transitions in lanthanum cobaltite perovskites as a function of temperature is presented. Specifically, the defect structure of LaCoO_3 based rhombohedral perovskites is characterized, a ferroelastic to paraelastic phase transition in $\text{La}_{0.6}\text{Ca}_{0.4}\text{CoO}_3$ is studied by in-situ high temperature TEM, and the microstructural changes occurring during thermal cycling are investigated. In the second part of the publication the stress-strain relationships and hysteresis in LaCoO_3 based perovskites studied by compression will be discussed.

2. Materials and experimental details

It was recently discovered that LaCoO_3 based perovskites have a ferroic character [21,23]. A ferroelastic transition is necessarily connected to a change in the crystal system and these ceramics exhibit cubic (a space group $Pm\bar{3}m$ stable at high temperature) to rhombohedral (a space group $R\bar{3}c$ stable at low temperature) gradual displacive phase transition (Fig. 1) [25]. The transformation between the cubic and non-centrosymmetric rhombohedral phases produces four distinct variants, which have unique deformation states with

respect to the prototype. The rhombohedral spontaneous deformation involves a stretching along one of four $[111]$ directions. The spontaneous ferroelastic strain in the rhombohedral LaCoO_3 perovskite is due to the rotation of the corner sharing CoO_6 -octahedra, which causes the Co-O-Co bond angle to be lower than 180° . The octahedra in the LaCoO_3 perovskite are flattened along the $[111]$ pseudocubic direction, which is the axis of rotation. It is convenient to use the rhombohedral angle α between the pseudo-cube $[101]$ direction for the description of the rhombohedral distortion. α is equal 60° in the case of cubic symmetry. For pure LaCoO_3 perovskite $\alpha = 60.79^\circ$ was reported [25]. Pure LaCoO_3 remains in the rhombohedral phase close to the melting point (1700°C) temperature [26,27]. The rhombohedral distortion of LaCoO_3 perovskite and the temperature of $c \rightarrow r$ transition can, however, be lowered by divalent cation substitution on the A site [22,25]. The rhombohedral distortion of pure LaCoO_3 perovskite is the highest possible from the crystallographic point of view and will be lowered by doping with A^{2+} (where A^{2+} can be Sr^{2+} , Ca^{2+} , or Ba^{2+}) cations on A site, until at the level of substitution of slightly above $x = 0.5$, the rhombohedral angle becomes equal 60° and the system becomes cubic. Thus, the transition temperature can be expected to be around 950°C for $\text{La}_{0.8}\text{Ca}_{0.2}\text{CoO}_3$ and around 700°C for $\text{La}_{0.6}\text{Ca}_{0.4}\text{CoO}_3$ perovskites [28,29].

Pure LaCoO_3 and Ca-doped $\text{La}_{0.6}\text{Ca}_{0.4}\text{CoO}_3$ and $\text{La}_{0.8}\text{Ca}_{0.2}\text{CoO}_3$ perovskites were produced by Praxair Surface Technologies, Specialty Ceramics. Single phase materials with no detectable secondary phases were determined by XRD. The average grain size of 2–5 micron was measured for all three compositions. A JEOL JEM-3010 TEM was used for the microstructural studies. High temperature in-situ experiments were performed on Ca-doped materials. A Gatan Model 652 double tilt heating stage, with a tantalum furnace, was used to heat perovskite foils up to 700°C at a controlled heating rate of 10 or 20°C per min. The oxygen partial pressure in the microscope column is about 5×10^{-8} Pa, therefore the perovskite sample is in a highly reducing atmosphere during the high temperature experiments [30].

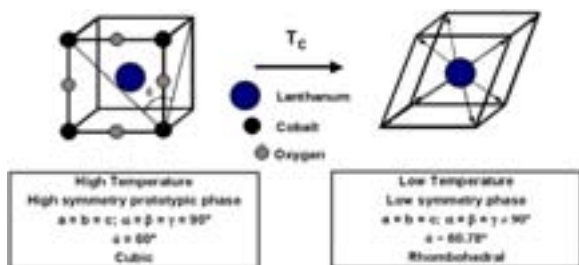


Fig. 1. Schematic presentation of the ferroelastic phase transition from cubic to rhombohedral phase in LaCoO_3 perovskite.

3. Results

3.1. Twins in LaCoO_3 based perovskites

Twins are the dominant structural feature of rhombohedral perovskites at room temperature. Different types of twins can be found, such as short parallel domains oriented at 180° to each other, wedge shaped twins, long lamellas, and herring bone structures were generally observed. We did not see the tweed structure or any trace of spinodal decomposition, which are other evidences of a paraelastic to ferroelastic transition [2].

Short parallel domains oriented at 180° relatively to each other as well as long lamellas in LaCoO_3 are shown in Fig. 2(A). The dominant morphological feature of these short parallel domains is that they are relatively straight and possess a high degree of 180° orientation with respect to each other. During the heating experiments these short 180° domains have been in the highly mobile state starting from 150°C , and they had a tendency to disappear at once at temperatures of $200\text{--}250^\circ\text{C}$ for $\text{La}_{0.6}\text{Ca}_{0.4}\text{CoO}_3$ compositions. Their movements during the heating have lead to bending and buckling of the sample. The electron diffraction pattern taken from the twin's area exhibits the splitting of the spots (Fig. 2(B)). The magnitude of the splitting increases with the distance from the center of the pattern. The splitting of the spots in the diffraction pattern reflects the lowering of the symmetry from cubic to rhombohedral during the

phase transition. Another example of short 180° twins along with wedge shaped domains that were observed in $\text{La}_{0.8}\text{Ca}_{0.2}\text{CoO}_3$ perovskite at 800°C are shown at Fig. 3. T_c of $\text{La}_{0.8}\text{Ca}_{0.2}\text{CoO}_3$ is 950°C [22] that is why a twin structure is significantly less mobile and more stable in the region of temperatures below 950°C in comparison to the $\text{La}_{0.6}\text{Ca}_{0.4}\text{CoO}_3$ domains.

Needle shaped domains were also observed in LaCoO_3 (Fig. 4, insert), which can easily be considered as twins. However there is no significant orientation change between adjacent domains, which exists in the twin structure. An HRTEM image of a domain wall (Fig. 4) shows that the boundaries are almost perfectly aligned with each other. No splitting of the selective area diffraction spots taken across the domain boundary has been observed. From these results, the lattice parameters of $a = 5.4445\text{\AA}$; $c = 13.0936\text{\AA}$ with an atomic spacing of $d = 3.94\text{\AA}$ in $[112]$ direction and $d = 3.78\text{\AA}$ in $[012]$ direction were calculated. The tilt angle of the domain wall was measured to be 177.89° . It is possible that this deviation from 180° is due to a shear deformation of twinning which occurs during the ferroelastic phase transformation. To answer the question about the nature of the domain wall, Z-contrast imaging should be used [30,31].

3.2. Stacking faults and dislocations in LaCoO_3 based perovskites

Another planar defects, besides twins, that were often observed were stacking faults (Fig. 5). They

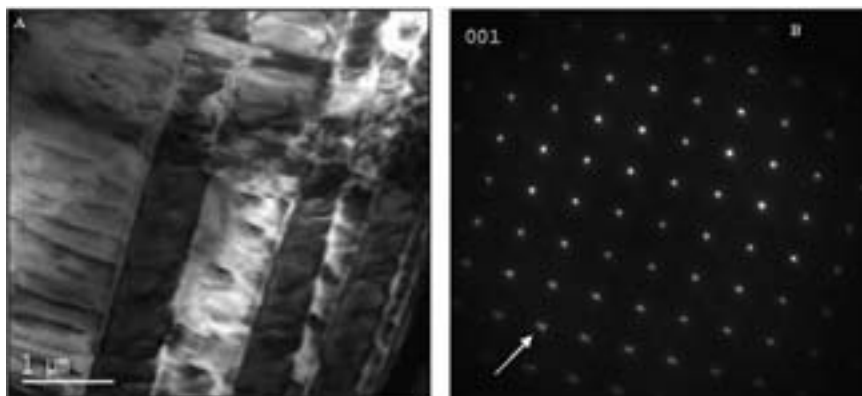


Fig. 2. (A) Bright field TEM micrograph of a typical twin structure in the pure LaCoO_3 perovskite. (B) SAD pattern from the area A. An arrow shows spot splitting due to the transformation from cubic to rhombohedral symmetry.

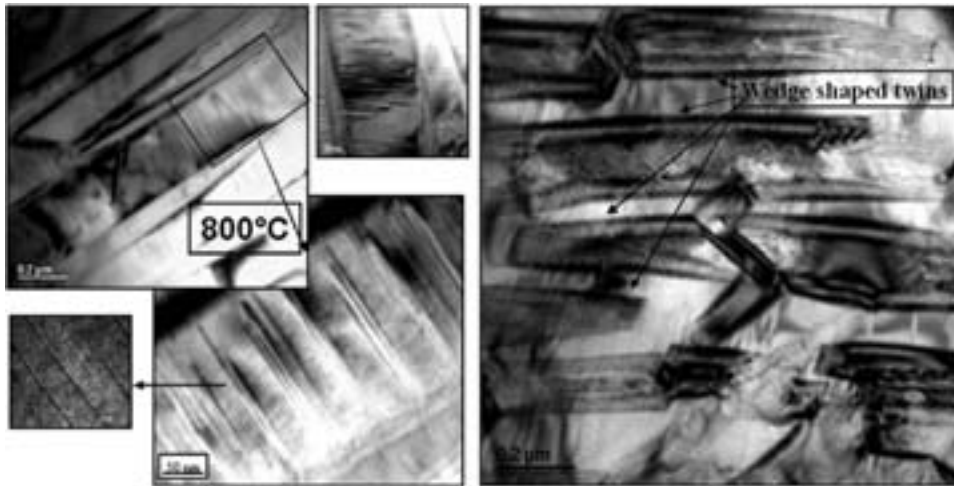


Fig. 3. Short parallel to each other twins along with wedge shaped twins are stable up to 850 °C in $\text{La}_{0.8}\text{Ca}_{0.2}\text{CoO}_3$ perovskite.

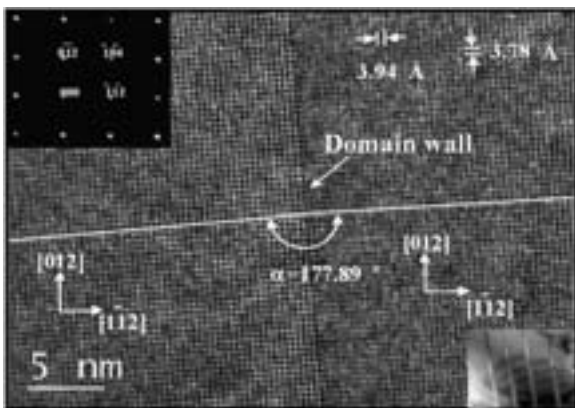


Fig. 4. Domain wall in LaCoO_3 .

appeared only after the sample was exposed to the reduced environment at high temperature in the microscope column. In the as-received sample no stacking faults have been observed. Once the stacking faults appeared upon cooling, they were able to move/shrink and disappear very fast during the further heating/cooling cycling. Such movement of stacking faults at high temperatures in reducing atmosphere (high vacuum of the TEM) can be connected to the oxygen vacancies formation in the LaCoO_3 lattice. The role of the stacking faults in domain switching/transformation mechanisms is not clear and more work is required to understand how and why they affect transition processes and

what is their input in the ferroelasticity phenomenon.

The dislocations could not be seen easily at room temperature, since they were hidden by overlapping twins and other defects. However, during the heating, when the other defects disappear, the dislocations can be observed. A dislocation in $\text{La}_{0.6}\text{Ca}_{0.4}\text{CoO}_3$ perovskite at 400 °C is shown in Fig. 5. These dislocations serve as strong pinning points for de-twinning process, thus preventing and delaying shrinkage and disappearance of the twins during heating (Fig. 6).

3.3. Dynamics of the ferroelastic phase transition in $\text{La}_{0.6}\text{Ca}_{0.4}\text{CoO}_3$

For the first time, the mobility of domains was recorded in-situ in the LaCoO_3 based perovskite using a high temperature (up to 850 °C) heating stage in the TEM. Heating allows one to directly identify changes from the static to dynamic twinning near the phase transition temperature, and to observe the de-twinning process during heating and reappearance of domains during cooling. The $\text{La}_{0.6}\text{Ca}_{0.4}\text{CoO}_3$ composition was chosen for the in-situ high temperature TEM experiments because of the maximum temperature restrictions (850 °C is a maximum) during the heating experiments as the T_c of the $\text{La}_{0.6}\text{Ca}_{0.4}\text{CoO}_3$ perovskite is around 700 °C [29]. Different steps of the de-twinning process

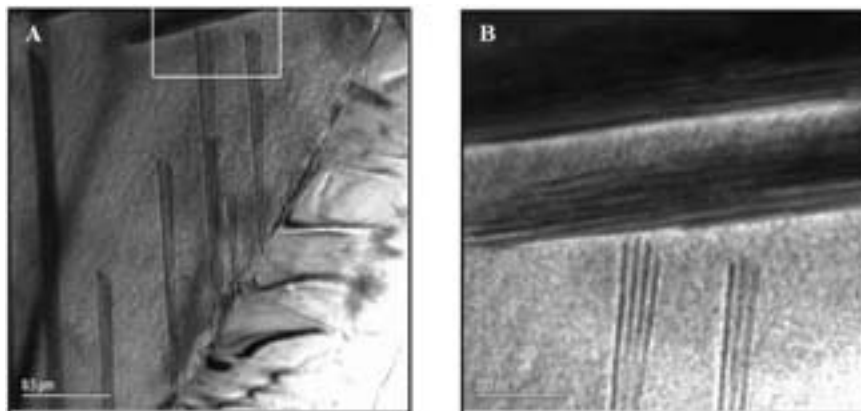


Fig. 5. (A) Stacking faults in $\text{La}_{0.6}\text{Ca}_{0.4}\text{CoO}_3$ perovskite observed by TEM at room temperature after dwelling of the sample at 700 °C for 10 mins. (B) A higher magnification image of the upper part of micrograph (A).

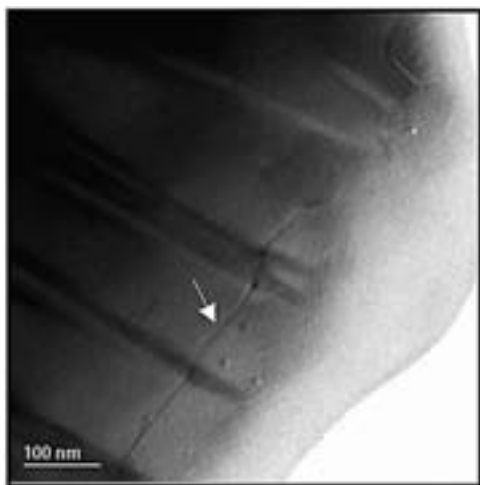


Fig. 6. Twins in $\text{La}_{0.6}\text{Ca}_{0.4}\text{CoO}_3$ perovskite at 400 °C. A dislocation (marked by arrow) is observed near the twins' tips. Some of the twins have bifurcated tips.

are shown in Fig. 7. Two types of domains can be generally observed on the as received TEM sample – 180° and $\sim 90^\circ$ domains [32]. Upon heating the 180° domains are found to be the most unstable and mobile, disappearing at 200–250 °C. Other long domains are stable up to 400 °C (Fig. 7(B)), they are not mobile and simply shrink when the temperature increases up to 700 °C. At this temperature dislocations can be observed and the grain is almost free from twins, i.e. it is a single domain grain (Fig. 7(C)). On cooling, the long twins

reappear almost at the same place and in the same position. After cooling, the long twin pattern corresponds to the one seen before heating, while the 180° twins did not return, i.e. the structure after cooling does not exactly correspond to the structure before heating (Fig. 8). The main difference was an appearance of stacking faults. Their formation possibly can be explained by the formation of oxygen vacancies during the reduction of the $\text{La}_{0.6}\text{Ca}_{0.4}\text{CoO}_3$ perovskite to the orthorhombic brownmillerite phase during heating in the highly reducing conditions of the microscope [33]. The origin of the stacking faults and their relationship with ordered oxygen deficient samples is one of the problems to be further studied.

Electron diffraction patterns taken during heating and cooling are very complicated and will be described elsewhere. Ordered structure, change of the diffraction pattern during phase transition/detwinning in real time, and the superstructure were recorded in-situ during the heating experiments. More thorough and detailed work is required to determine the crystal structure (d spacing, growth direction, ordering, superstructure indexing, etc.) during the heating cycles of LaCoO_3 based perovskites. This investigation of the twinning/detwinning process, domain wall motion and thickening will lead us to a new level of understanding of the effect of the microstructure on the stability of LaCoO_3 based perovskites.

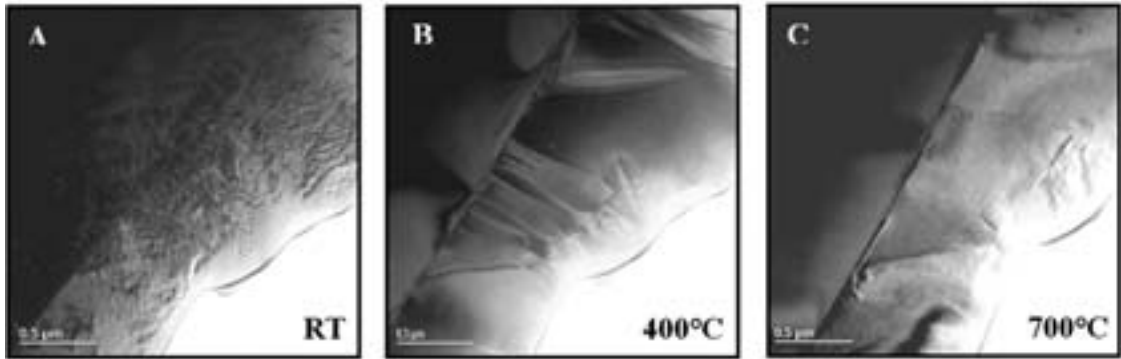


Fig. 7. The sequence of micrographs showing dynamics of the de-twinning upon heating. (A) Multidomain state in as-prepared structure at room temperature before heating; (B) Long domains are stable at 400 °C; (C) Single domain grains exist at 700 °C.

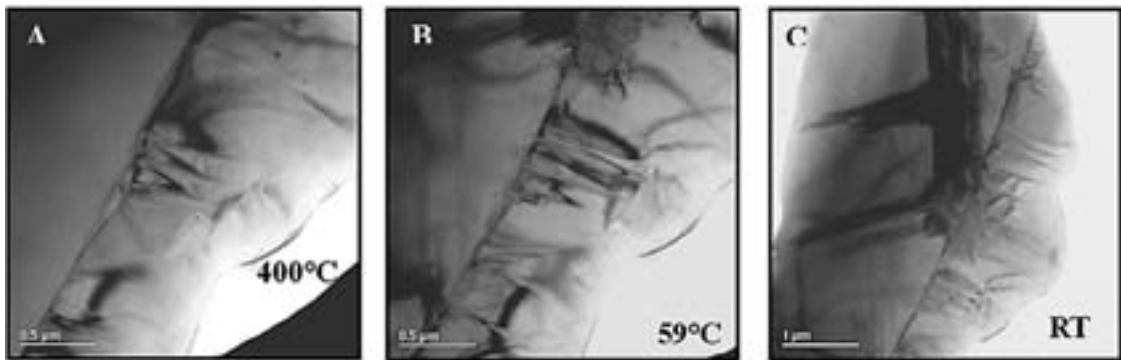


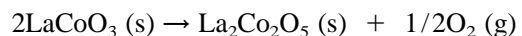
Fig. 8. The sequence of micrographs showing the re-appearance of twins during cooling (A) Re-appearance of long twin lamellas during the cooling at 400 °C. Long twins are growing at the same position, as they existed before heating; (B) At the end of cooling, long twins reached the same size as before heating. The multidomain state, which existed on as-received foil, did not re-appear. (C) The huge twin bands re-growth during the cooling. The formation of such twins leads to bending and cracking of the perovskite foil upon cooling and appearance of considerable residual strains.

3.4. Annealing of perovskite samples at high temperature

The same specimen of $\text{La}_{0.6}\text{Ca}_{0.4}\text{CoO}_3$ was reheated to 700 °C and then annealed at this temperature for a period of time. The bending and strain generated during the previous thermal cycle had reduced the number of areas that could be looked at in this experiment. A micrograph of one of these grains was taken at 700 °C, immediately after heating (Fig. 9(A)) and after 25 mins at 700 °C (Fig. 9(B)). As expected, upon reaching 700 °C, most of twins and twin related defects disappeared and the grain became a single domain grain. However, when held at 700 °C for 25 mins, a further trans-

formation occurred including the appearance and movement of new stacking faults.

It is known that LaCoO_3 perovskite is easily reduced and can undergo topotactic, low temperature reduction to vacancy-ordered phase [34]



An orthorhombic brownmillerite-type structure was reported for $\text{LaCoO}_{2.5}$ [35], which consists of alternate layers of Co in octahedral and tetrahedral sites. The structure was described as the perovskite-type structure with every second row of oxygen atoms being removed from alternate planes [34]. The phase transition and appearance and movement of stacking faults observed during annealing

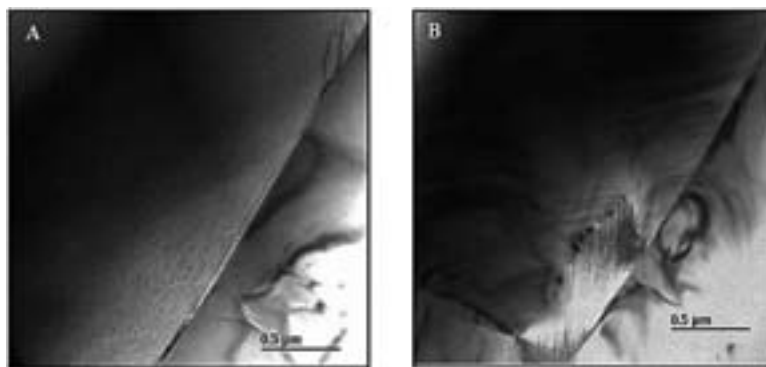
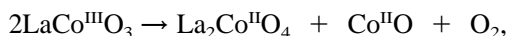


Fig. 9. TEM micrographs of $\text{La}_{0.6}\text{Ca}_{0.4}\text{CoO}_3$ perovskite at 700 °C. (A) Micrograph taken immediately after heating. A single domain grain can be clearly seen. (B) Micrograph taken after 25 min of annealing at 700 °C.

at 700 °C can be connected to the reduction and oxygen vacancies formation in $\text{LaCoO}_{2.5}$ structure. We did not observe any formation of cobalt oxides during the annealing at 700 °C of $\text{La}_{0.6}\text{Ca}_{0.4}\text{CoO}_3$.

Heating and dwelling at 800 °C experiments on $\text{La}_{0.8}\text{Ca}_{0.2}\text{CoO}_3$ perovskites ($T_c = 950$ °C) did not lead to the temperature induced ferroelastic phase transition and twin structure remained stable at 800 °C for this composition. This can be explained by low mobility of domains walls comparable to those in $\text{La}_{0.6}\text{Ca}_{0.4}\text{CoO}_3$. We found that Co_3O_4 with a spinel structure was formed on the surface of $\text{La}_{0.8}\text{Ca}_{0.2}\text{CoO}_3$ perovskite sample during annealing experiments at 800 and 850 °C [36] (Fig. 10). We did not detect any deficiency of cobalt in the perovskite grains or grain boundary, even though such

deficiency should exist. The reduction process of LaCoO_3 can be written as



$\text{Co}_3^{\text{II,III}}\text{O}_4$ is an intermediate product of the reduction process. Depending on temperature and oxygen pressure this reduction may terminate in the formation of metallic cobalt.

4. Conclusions

A TEM study of the ferroelastic domain configuration and phase transition of rhombohedral

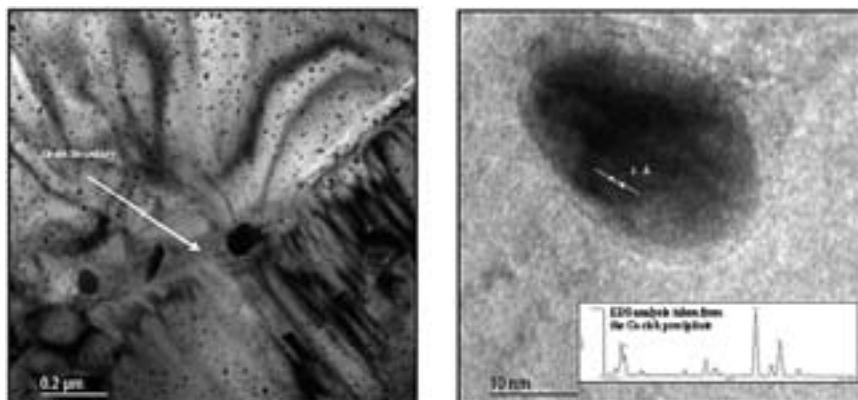


Fig. 10. Co_3O_4 surface precipitations during annealing of $\text{La}_{0.8}\text{Ca}_{0.2}\text{CoO}_3$ for 1.5 hr at 800 °C. Precipitation is favored along the grain boundaries of perovskites.

LaCoO₃ based ceramics has been carried out. Twins, stacking faults and dislocations were observed in LaCoO₃ based perovskites. For the first time, the mobility of domains was recorded in-situ by high temperature TEM in the La_{0.6}Ca_{0.4}CoO₃ perovskite, which allows one to directly identify change from the static to dynamic twinning near the phase transition temperature, and to observe the de-twinning process during the heating and reappearance of domains during cooling. Thus, the origin of the ferroelastic behavior of these materials has been demonstrated. Annealing of the La_{0.6}Ca_{0.4}CoO₃ specimen above $c \rightarrow r$ transformation temperature leads to progressive transition and formation of new stacking faults, which can be connected to the formation of oxygen deficient brownmillerite-type LaCoO_{2.5} structure. Annealing of the La_{0.8}Ca_{0.2}CoO₃ specimen at 800 °C for 1.5 hrs leads to the surface formation of the cobalt oxide precipitations.

Acknowledgements

The financial support of the National Science Foundation through Grant number DMR-0201770 is acknowledged. We would like to thank Daibin Ge, Drexel University for help with lattice parameters calculations of LaCoO₃ perovskite.

References

- [1] Aizu K. J Phys Soc Japan 1969;27:387.
- [2] Salje EKH. Phase transitions in ferroelastic and co-elastic crystals. Cambridge: Cambridge University Press, 1990.
- [3] Kriven WM. In: Yoo MH, Wuttig M, editors. Twinning in advanced materials. Warrendale, PA: TMS; 1994, p. 435.
- [4] Wadhawan V. Phase transitions 1982;3:3.
- [5] Aizu K. J Phys Soc Japan 1969;7:387.
- [6] Metrat G. Ferroelectrics 1980;26:801.
- [7] Balachandran U, Dusek JT, Sweeney SM, Poeppel RB, Mieville RL, Maiya PS et al. Am Ceram Soc Bull 1995;74:1.
- [8] Minh NQ. J Am Ceram Soc 1993;76:563.
- [9] Teraoka Y, Nobunaga T, Yamazoe N. Chem Lett 1988:503.
- [10] Mizusaki J, Yoshihiro M, Yamauchi S, Fueki K. J Solid State Chem 1985;58:257.
- [11] Heikes RR, Miller RC, Mazelsky R. Physica 1964;30:1600.
- [12] Bhide VG, Rajoria DS, Rama Rao G, Rao CNR. Phys Rev B 1972;6:1021.
- [13] Yamaguchi S, Okimoto Y, Taniguchi H, Tokura Y. Phys Rev B 1995;52:11681.
- [14] Sehlin SR, Anderson HU, Sparlin DM. Phys Rev B 1995;52:11681.
- [15] Raccah PM, Goodenough JB. Phys Rev 1967;155:932.
- [16] Thornton G, Morrison FC, Partington S, Tofield BC, Williams DE. J Phys C 1988;21:2871.
- [17] Asai K, Yokokura O, Nishimori N, Chou H, Tranquada JM, Shirane G. Phys Rev B 1994;50:3025.
- [18] Maiya PS, Balachandran U, Dusek JT, Mieville RL, Kleefisch MS, Udovich CA. Solid State Ionics 1997;99:1.
- [19] Kim S, Yang YL, Christoffersen R, Jacobson AJ. Solid State Ionics 1998;109:187.
- [20] Goldberg E, Nemudry A, Boldyrev V, Schoellhorn R. Solid State Ionics 1998;110:223–233.
- [21] Orlovskaya N, Gonzalez N. J Materials Processing and Manufacturing Science 2000;9:53.
- [22] Kleveland K, Orlovskaya N, Grande T, Moe A-M, Einarsrud M-A, Breder K, Gogotsi G. J Am Ceram Soc 2001;84:2029.
- [23] Orlovskaya N, Gogotsi Y, Reece M, Cheng B, Gibson I. Acta Mater 2002;50:715.
- [24] Kato T, Momma A, Nagata S, Kasuga Y. J Ceram Soc Jap 1997;105:1142.
- [25] Ravindran P, Korzhavyi PA, Fjellvag H, Kjekshus A. Phys Rev B 1999;60:16423.
- [26] Coutures J-P, Badie JM, Berjoan R, Coutures J, Flamand R, Rouanet A. High Temp Sci 1980:331.
- [27] Gilbu B, Fjellvag H, Kjekshus. Acta Chem Scand 1994;48:37.
- [28] Thornton G, Tofield BC, Hewat AW. J Solid State Chem 1986;61:301.
- [29] Orlovskaya N, Gogotsi Y, Nicholls A. Proceedings of 7th Int Symp On Solid Oxide Fuel Cells, Yokokawa H, Singhal SC, editors. 2001, p. 624.
- [30] Klie RF, Ito Y, Stemmer S, Browning ND. Ultramicroscopy 2001;86:289.
- [31] Ito Y, Klie R, Browning N, Mazanec T. J Am Ceram Soc 2002;85(4):969–976.
- [32] Floquet N, Valot CM, Mesnier MT, Niepce JC, Normand L, Thorel A, Kilaas R. J Phys III France 1997;7:1105.
- [33] Van Doorn RHE, Burggraaf AJ, Solid State Ionics 2000;128:65.
- [34] Tilset BG, Fjellvag H, Kjekshus A. J Sol State Chem 1995;119:271.
- [35] Vidyasagar K, Reller A, Gopalakrishnan J, Rao CNC. J Chem Soc Chem Commun 1985:7.
- [36] Orlovskaya N, Ge D, Nicholls A. Key Engineering Materials 2001:206.